MASS TRANSPORT THROUGH INTERSTITIAL STRUCTURES

B. IWANOWSKA-CHOMIAK[*]
University Hospital of Zielona Góra, Oncology Department
ul. Zyty 26, 65-046 Zielona Góra, POLAND
E-mail: B.Chomiak@op.pl

A. WALICKA
University of Zielona Góra
Szafrana Str. 4, POLAND
E-mail: A.Walicka@ibem.uz.zgora.pl

Interstitial space, also called interstitum, separating the vital organs of a human body, is the primary source of lymph and is a major fluid compartment in the body.

Interstitial space (IS) is filled out by thick collagen (CL) bundles which form lattices represented by a network of capillaries. This network has the structure similar to a sponge porous matrix (SPM) with pores-capillaries of variable cross-section.

To analyse the mass transport of interstitial fluids (IFs) through the porous matrix it is assumed that the SPM is composed of an irregular system of pores which may be modelled as a fractal porous matrix. The interstitial fluids can be either bio-suspensions or bio-solutions and therefore they have to be modelled as non-Newtonian fluids. Analysing the fluid flow through the porous matrix it is assumed that the SPM is modelled as capillary tubes of variable radii. Introducing a hindrance factor allowed us to consider the porous matrix as a system of fractal capillaries but of constant radii.

Classical and fractal expressions for the flow rate, velocity and permeability are derived based on the physical properties of the capillary model of interstitial structures. Each parameter in the proposed expressions does not contain any empirical constant and has a clear physical meaning, and the proposed fractals models relate the flow properties of the fluids under consideration with the structural parameters of interstitium as a porous medium.

Key words: interstitial space, interstitial fluids, fractal models.

1. Introduction

All tissues and organs contain a mixture of cells and non-cellular components, which form bio-networks called extracellular matrices (ECMs). These matrices provide not only bio-mechanical scaffolds into which cells are embedded but also regulate many cellular and intercellular processes such as growth, migration, differentiation, survival, homeostasis and morphogenesis [1-4]. The ECMs consist of a large variety of matrix macromolecules whose precise composition and specific structures vary from tissue to tissue. The major constituents of ECMs are fibrous forming proteins such as collagens (CLs), elastin (EL), fibronectin (FN), laminins (LAs), glycoproteins (GPs), proteoglicans (PGs) and glycosaminoglycans (GAGs) which are highly acidic and hydrated molecules.

ECMs can be classified into two major types that vary in composition and structure: the interstitial and pericellular matrices; the interstitial matrices (ISMs) surround cells, whereas the pericellular matrices (PCMs) are in close contact with cells [4].

---

* To whom correspondence should be addressed

The latest research indicates that interstitial structures create probably one of the largest organs of the human body [5-7]. They are present in all body; Fig.1 shows schematically the location of identical histologic structures seen in fibroconnective tissues throughout the body.
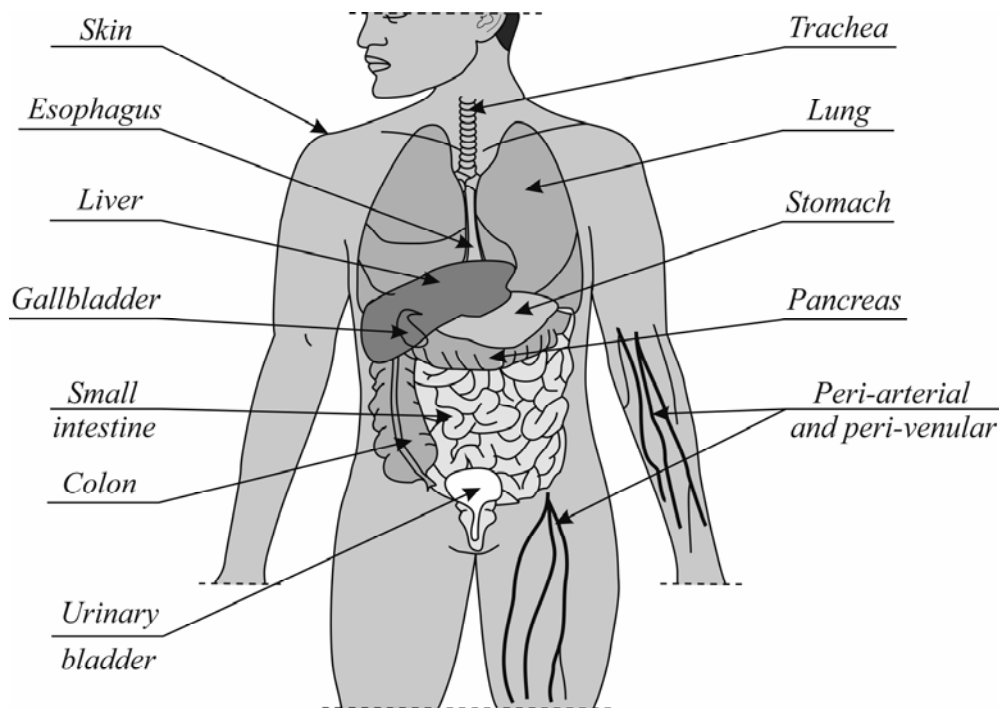
Fig.1. Schematic location of an interstitial space.

The interstitial space, also called interstitium, is the primary source of lymph and is a major fluid compartment in the body [6]. The interstitium is a fluid-filled space existing between a structural barrier such as cell walls or the skin and internal structures such as organs including muscles and the circulatory system [7]. The fluid in this space - called interstitial fluid (IF) - comprises water and solutes, and drains into the lymph system [8].

The non-fluid parts of the interstitium are predominanty collagens (CLs) of type: I, III and V, elastin (EL) and glycosaminoglycans (GAGs) such as hyaluronate (HA) and proteoglycans (PGs) that are cross-linked to form a honeycomb-like reticulum [9-12]. Such structural components exist both for the general interstitium of the body [6-8] and within individual organs such as e.g., the heart and kidney [9, 13].

The interstitial fluid is a reservoir and transportation system for nutrients and solutes distributing among organs, cells and capillaries for signaling molecules communicating between cells and for antigens and cytokines participating in immune regulation [8]. This fluid flowing across the capillary walls must cross the interstitial spaces between parenchymal cells to gain access to the lymphatic vasculature and to the vascular system. The interstitium does not simply represent a passive conduit system for the flux of fluid and solutes but also functions as a highly dynamic and complex structure whose physical properties exert profound influences on the fluid and solute exchange and the behaviour of tissue cells. Capillary filtration drives the fluid through the interstitium which is essential for proteins transport from the blood to parenchymal and interstitial cells because these macromolecules are too large to readily diffuse through the ensemble of extracellular matrix components that fill the space between the vascular and lymphatic micro-systems [4]. The composition and chemical properties of the interstitial fluid vary among organs and undergo changes in chemical composition during normal function as well as during body growth or, for instance, conditions of inflammation and development of diseases such as heart failure or chronic kidney disease [6-8].

The total fluid volume of the interstitium in a healthy man is about *20*% of body mass but this quantity is dynamic and may change in volume and chemical composition during immune responses and in conditions such as cancer and specifically within the interstitium of tumors. The amount of the interstitial fluid varies from about *10*% in skeletal muscle to about *50*% of the tissue mass in skin [8].

It may be hypothesised that the interstitial space is filled out by thick collagen bundles which form complex lattices representing a network of capillaries or lymphangioles. This network has the structure similar to a sponge porous matrix (SPM) [7] and it is schematically presented in Fig.2.
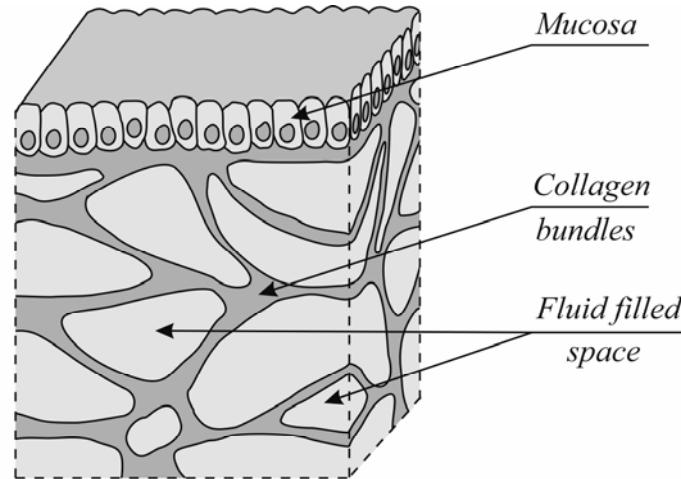
Fig.2. Schematic model of a sponge porous matrix (MSPM).

One suggests that this network of capillaries may serve for the transport of circulating tumor cells (CTCs) which are cancer cells that shed from a primary tumor and circulate in the interstitial structure [14]. Note that cancer is the leading cause of death worldwide and metastasis is responsible for more than *90*% of the mortality of cancer patients [15].

Metastasis occurs when tumor cells leave the primary tumor, travel through the blood or lympha steam as CTCs, and then colonize secondary tumors at sites distant from the primary tumor. Since the discovery of CTCs in 1869 by Ashworth [14], researchers have utilized CTCs for the early detection of aggressive cancer and the treatment of advanced disease. CTCs are extremely rare - approximately one CTC is mixed with one million (10^6) of leucocytes or one billion (10^9) of erythrocytes - in circulating blood and their detection is possible using the techniques of high specificity and high sensitivity [14, 15]. The rarity of CTCs has not any effect on the mass transport through the interstitial structure but the knowledge on flows of interstitial fluids is very essential to the detection of CTCs.

The aim of this work is to present general analytical methods for deriving mathematical relations between interstitial fluid pressure (IFP) losses and the volumetric flow rate for laminar flows of IFs in a porous medium such as the interstitial structure. This structure is modelled as the sponge porous matrix (Fig.2) when capillary tubes are tortuous and of variable cross-section (e.g.: convergent - divergent; see Fig.3a). The flows through interstitial structures are analysed twofold: as classical flows or as fractal flows [16, 17]. The interstitial fluids are modelled as Newtonian fluids (it is acceptable as the first order approximation for the case of a healthy human organism) or as non-Newtonian fluids (for all other cases).

2. Classical flows through the interstitial structures

In what follows we will consider the classical models of flow through the interstitial structures considered as a sponge porous matrix (SPM) composed of capillary tubes. Assuming that the capillaries are tortuous and have variable cross-sections, we will present the formulae for the flow of the following fluids:

Newtonian, generalized viscoplastic (Shulman model), pseudoplastic (DeHaven and Sisco model) and polar fluids (micropolar and couple-stress) [16, 18]. Detailed mathematical considerations can be found in [16, 17, 19-22].

These considerations will be successively supplemented by deliberations on the capillary tortuosity and variability of cross-section (see Fig.3a).

The tortuosity of capillaries may be defined by a tortuosity factor being the ratio of actual capillary tube length L_T to the thickness (length) L_0 of the porous layer

$$T = \frac{L_T}{L_0} \tag{2.1}$$

where T is the tortuosity factor.

Next notion is the porosity of a porous medium which is defined by the following relation

$$\varphi_p = \frac{V_p}{V} \qquad \text{or} \qquad \varphi_p = \frac{A_p}{A} \tag{2.2}$$

where: V is the total volume of the porous medium, V_p is the total volume of open pores; A is the total area of the sample cross-section (see Fig.2.), A_p is the total pore area of the considered sample.

The last notion is the hindrance factor connected with the following property of the porous medium, i.e., the real volumetric flow through the pores of variable cross-section is less than the (theoretic) flow through the pores modelled as capillaries of constant cross-section. This factor is defined by the ratio

$$\psi = \frac{Q_v}{Q_t} \tag{2.3}$$

where: Q_v is the real flow rate through capillary of variable cross-section, Q_t is the theoretic flow rate through capillary of constant cross-section.

Introduction of the hindrance factor allows us to evade not always possible but always tedious calculations [19-22].

2.1. Newtonian fluids

Newtonian fluids may model - in the first approximation - all flows through the lymph system of the healthy human body.

The average flow velocity through the porous matrix (Fig.3a) of a Newtonian fluid is given as follows (Fig.3b)

$$\upsilon_N = \frac{r_c^2 \varphi_p \psi_N}{8\mu T} \left(-\frac{dp}{dy} \right) \tag{2.4}$$

where r_c is the constant capillary radius, φ_p is the porosity of the porous matrix, ψ_N is the hindrance factor for Newtonian fluids flow, μ is the Newtonian viscosity T is the tortuosity factor (only for tortuous capillary tubes); here: $1 \leq T \leq 2$; note that

$T=1$ for straight capillary,

$T>1$ for tortuous capillary.

The term dp/dy denotes the pressure gradient which may be replaced by the local thrust provoked on the mucosa by the surrounding environment; thus we have

$$-\frac{dp}{dy} = \frac{\Delta p}{h} \tag{2.5}$$

where Δp is the local thrust, h is the thickness of the interstitial structure (porous layer).
Therefore (2.4) may be written in the following form
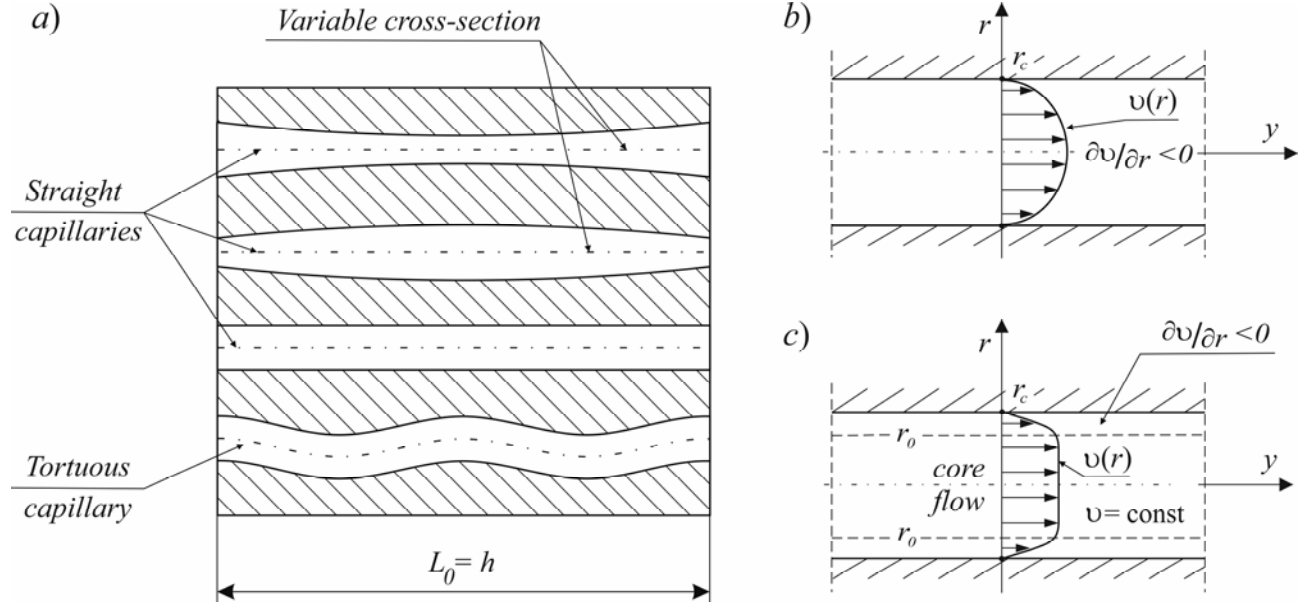
Fig.3. Porous matrix composed of rectilinear parallel capillary tubes (a); capillary tube with Newtonian fluid flow (b), capillary tube with Shulmanian fluid flow (c).

$$\upsilon_N = \frac{r_c^2 \varphi_p \psi_N \Delta p}{8\mu Th} \tag{2.6}$$

whereas the total amount of the lymph which is transported through the interstitial surface of an area A is equal to

$$Q_N = \frac{ANr_c^2 \varphi_p \psi_N \Delta p}{8\mu Th} \tag{2.7}$$

where Q_N is the total flow rate of the Newtonian fluid, N is the number of capillary tubes on the area A of the porous matrix.

2.2. Generalized viscoplastic fluids of a Shulman type

These fluids may model more exactly the lymph flows with many biological agents and also the blood flows with different therapeutic substances.

To analyse the flows of generalized viscoplastic fluids the model of a Shulman fluid is often used. This model - in one dimensional form - and the other simpler models of viscoplastic fluids derived from the Shulman model are presented in Tab.A.1 (see Appendix) [16-18]. The full analysis of the flows of these fluids can be found in [16, 19]. The flow field of a viscoplastic fluid in a capillary tube is shown in Fig.3c. The average velocity flow of this fluid in a capillary tube of constant cross-section is given as follows [17]

$$\upsilon_{Sh} = T^{(m)}_{(n)} \frac{r_c^{\frac{m+n}{n}}}{2^{\frac{m}{n}} \mu} \left(-\frac{dp}{dy}\right)^{\frac{m}{n}} \tag{2.8}$$

where: m, n are the flow behaviour indices, μ is the plastic viscosity and

$$T^{(m)}_{(n)} = \Upsilon^{\frac{m+3n}{n}} \sum_{i=0}^{m} (-1)^i \frac{n}{m+3n-i} C_m^i \left(\Upsilon^{-\frac{m+3n}{n}} - 1\right) \tag{2.9}$$

whereas

$$\Upsilon = \frac{r_0}{r_c}, \qquad C_m^i = \frac{m!}{i!(m-i)!}, \qquad m! = 1 \cdot 2 \cdot 3 \cdot ... \cdot m. \tag{2.10}$$

Introducing into (2.8) the hindrance factor ψ_{Sh} and the tortuosity factor T we may write the following formula for the velocity flow through a porous matrix composed of the capillaries of variable cross-section

$$\upsilon_{Sh} = T^{(m)}_{(n)} \frac{r_c^{\frac{m+n}{n}} \varphi_p \psi_{Sh}}{(2T)^{\frac{m}{n}} \mu} \left(-\frac{dp}{dy}\right)^{\frac{m}{n}}; \tag{2.11}$$

it may be assumed for the rectilinear capillary tubes of variable cross-section that

$$\psi_{Sh} = (\psi_N)^{\frac{m}{n}}. \tag{2.12}$$

For a special case of a Shulman fluid, when $n = 1$, $r_0 = 0$ (there is no core flow), we deal with an Ostwald-de Waele (power-law) fluid and then

$$T^{(m)}_{(1)} = \frac{1}{m+3}. \tag{2.13}$$

Note that for flows with a large core, $\Upsilon \approx 1$ and for flows with a small core when $\Upsilon \ll 1$, one can use the following approximations:
– for a large core

$$T^{(m)}_{(n)} \approx -\Upsilon^{\frac{m+3n}{n}} \sum_{n}^{m} (-1)^i \frac{n}{m+3n-i} C_m^i = -\Upsilon^{\frac{m+3n}{n}} \frac{(-1)^m}{3C_{m+3n}^m}, \tag{2.14}$$

– for a small core

$$T_{(n)}^{(m)} \approx \frac{n}{m+3n}\left[1 - \frac{m(m+3n)}{m+3n-1}\Upsilon^{\frac{1}{n}}\right]. \tag{2.15}$$

Note that these formulae are important for all fluids derived from the Shulman fluid, namely: for the Casson fluid $(m=n)$, Vočadlo fluid $(m=1)$, Herschel-Bulkley fluid $(n=1)$ and Bingham fluid $(m=n=1)$ and they are presented in Tab.1.

Table 1. Formulae for $T_{(n)}^{(m)}$ for the fluids derived from the Shulman fluid.

Fluid	Large core	Small core
Casson $m=n$	$\dfrac{(-1)^{n+1}}{3C_{4n}^{n}}\Upsilon^{4}$	$\dfrac{1}{4}\left[1 - \dfrac{4n^{2}}{4n-1}\Upsilon^{\frac{1}{n}}\right]$
Vočadlo $m=1$	$\dfrac{1}{3(3n+1)}\Upsilon^{\frac{3n+1}{n}}$	$\dfrac{n}{3n+1}\left[1 - \dfrac{3n+1}{3n}\Upsilon^{\frac{1}{n}}\right]$
Herschel-Buckley $n=1$	$\dfrac{(-1)^{m+1}}{3C_{m+3}^{m}}\Upsilon^{m+3}$	$\dfrac{1}{m+3}\left[1 - \dfrac{m(m+3)}{m+2}\Upsilon\right]$
Bingham $m=n=1$	$\dfrac{1}{12}\Upsilon^{4}$	$\dfrac{1}{4}\left[1 - \dfrac{4}{3}\Upsilon\right]$

Note that in medical applications all these approximations above are important only for m, n being odd numbers ($m, n = 1, 3, ...$).

Taking into account formula (2.7) and (2.12) we may now write the following equation for the total amount of the Shulman fluid in the flow through the interstitial surface of an area equals to A

$$Q_{Sh} = ANr_c^{\frac{m+n}{n}}\varphi_p\left(\frac{\psi_N\Delta p}{2Th}\right)^{\frac{m}{n}}T_{(n)}^{(m)} \tag{2.16}$$

where Q_{Sh} is the total flow rate of the Shulman fluid.

2.3. Pseudoplastic fluids

We will consider two essential models of these fluids, namely: DeHaven and Sisko fluid; many well-known but more complicated models reduce - for suitable selected material coefficients - either to DeHaven or to Sisko fluids. These models - in one dimensional forms - and similar models are presented in Tab.A.2 and Tab.A.3, respectively (see Appendix) [16-18].

The viscosity of a DeHaven fluid displays a non-linear relationship between the shear stress and the shear strain rate. To be more precise, the shear strain rate is a non-linear function of the shear stress. This fluid is characterised by a shear viscosity μ, which is similar to the Newtonian viscosity, material coefficient k_i and power exponent n_i, which represent aforementioned non-linearity of the shear strain rate.

The averaged flow velocity through a porous matrix composed of the capillaries of variable cross-section is given as follows [16, 17]

$$\upsilon_{DH} = \frac{r_c^2 \varphi_p \psi_N}{8\mu T} \left(-\frac{dp}{dy}\right) \left[1 + \frac{4k_i \psi_A}{\mu(n_i+4)} \left(\frac{r_c}{2T}\right)^{n_i} \left(-\frac{dp}{dy}\right)^{n_i} \right]. \tag{2.17}$$

The total flow rate through the area *A* of the interstitial structure is as follows

$$Q_{DH} = \frac{ANr_c^2 \varphi_p \psi_N \Delta p}{8\mu T\, h} \left[1 + \frac{4k_i \psi_A}{\mu(n_i+4)} \left(\frac{r_c}{2T}\right)^{n_i} \left(\frac{\Delta p}{h}\right)^{n_i} \right]. \tag{2.18}$$

Here ψ_A is the additional hindrance factor.

The viscosity of a Sisko fluid displays a non-linear relationship between the shear stress and the shear strain rate. This fluid is characterised by a shear viscosity μ which is similar to the Newtonian viscosity, the additional viscosity μ_i and power exponent n_i.

The flow velocity through the porous matrix composed of the capillaries of variable cross-section is given as follows [16, 17]

$$\upsilon_s = \frac{r_c^2 \varphi_p \psi_N}{8\mu T} \left(-\frac{dp}{dy}\right) \left[1 - \frac{4\mu_i \psi_s}{\mu(n_i+4)} \left(\frac{r_c}{2\mu T}\right)^{n_i} \left(-\frac{dp}{dy}\right)^{n_i} \right] \tag{2.19}$$

where ψ_s is the additional hindrance factor.

The total flow rate through the area *A* of the interstitial structure is given by following formula

$$Q_s = \frac{ANr_c^2 \varphi_p \psi_N \Delta p}{8\mu T\, h} \left[1 - \frac{4\mu_i \psi_s}{\mu(n_i+4)} \left(\frac{r_c}{2\mu T}\right)^{n_i} \left(\frac{\Delta p}{h}\right)^{n_i} \right]. \tag{2.20}$$

Note that both these models of pseudoplastic fluids render it possible - for respectively chosen material parameters: μ, k_i, μ_i, n_i - to consider the interstitial fluids with different biological additives and agents.

2.4. Polar fluids

These fluids are characteristic for all interstitial fluids being suspensions composed of particles having mean value of molecular weight, so they may model the flows of lymph and blood in a thinning state (e.g. after using some cardiological drugs).

Let us consider at first micropolar fluids. These fluids are described by two viscosities: the first of them is similar to the Newtonian shear viscosity μ, the other one, *k,* is the vortex (coupling) viscosity describing the particle rotation [16].

For the interstitial structure being a matrix composed of a large number of capillary tubes the flow velocity is given as follows (see Appendix) [16, 17]

$$\upsilon_m = \frac{r_c^2 \varphi_p \psi_N}{8\mu T} \left(\frac{\mu}{\mu+k}\right) \left(-\frac{dp}{dy}\right). \tag{2.21}$$

The amount of the micropolar fluid in the flow through the interstitial surface of an area *A* is equal to

$$Q_m = \frac{ANr_c^2 \varphi_p \psi_N \Delta p}{8\mu Th} \left(\frac{\mu}{\mu + k} \right).$$

(2.22)

Let us now consider the flow of a couple-stress fluid in the matrix composed of capillary tubes. The couple-stress fluid is composed of a mother fluid and rotated (in general) suspended particles.

This fluid is described by three viscosities: the first of them is a well-known Newtonian shear viscosity μ, the second ones, η and η', are connected with an existence of so-called couple-stresses and their influence on the fluid flow; these stresses result from the rotation of particles suspended in the mother fluid.

For the interstitial structure represented by a matrix with a large number of capillary tubes we have [16]

$$\upsilon_{cs} = \frac{r_c^2 \varphi_p \psi_N}{8\mu T} \left[1 - \frac{4l^2}{r_c^2} \left(1 - \frac{\eta'}{\eta} \right) \right] \left(-\frac{dp}{dy} \right)$$

(2.23)

where

$$l = \left(\frac{\eta}{\mu} \right)^{1/2},$$

(2.24)

is a material constant having the dimension of length.

If $\eta' \ll \eta$, then

$$\upsilon_{cs} = \frac{r_c^2 \varphi_p \psi_N}{8\mu T} \left(1 - \frac{4l^2}{r_c^2} \right) \left(-\frac{dp}{dy} \right).$$

(2.25)

In a special case when $\dfrac{r_c}{l} \approx 1$ and $\eta' \approx \eta$, then

$$\upsilon_{cs} = \frac{r_c^2 \varphi_p \psi_N}{8\mu T} \left[1 - 8(\eta - \eta')^2 \right] \left(-\frac{dp}{dy} \right).$$

(2.26)

This formula may be used to describe the blood flow in capillarity vessels.

The total flow rate is equal to

$$Q_{cs} = \frac{ANr_c^2 \varphi_p \psi_N \Delta p}{8\mu TL} \left[1 - \frac{4l^2}{r_c^2} \left(1 - \frac{\eta'}{\eta} \right) \right].$$

(2.27)

Note that for two left cases when $\eta' \ll \eta$ and $\eta' \approx \eta$ all formulae will be similar.

3. Fractal flows through interstitial structures

Fractal is a natural phenomenon or geometric set that exhibits a repeating pattern at every scale. It is also known as evolving or expanding geometry [16, 17]. Fractal geometry was popularized by Mandelbrot [23] when he showed that for a decreasing unit of measurement the length of a natural coastline does not converge but, instead, increases monotonically. His study on the length of the coastline, being scale-dependent, marked the origins of fractal geometry which has now found numerous applications in

characterizing and describing disordered phenomena in science and engineering (Mandelbrot [24]). More information on the engineering fractals applications may be found in the monograph [16].

Euclidean geometry describes objects such as points, curves surfaces and cubes using integer dimensions: 0, 1, 2 and 3, respectively. Measures of the object such as: the length of a line, the area of a surface and the volume of a cube are associated with each dimension. These measures are invariant with respect to the unit used to measurement. However, numerous objects found in nature [24] such as rough surfaces, porous media, coastlines, mountains, rivers, lakes and islands are disordered and irregular, thereby they do not follow the Euclidean description due to the scale - dependent measures. These objects are exactly called fractals and their dimensions are non-integral being defined as fractal dimensions.

The measure $M(L)$ of a fractal object is related to the length scale L by a scaling law in the following form [24]

$$M(L) \sim L^F \tag{3.1}$$

where F is the fractal dimension of an object.

Porous media in nature and also in medicine have been shown to be fractal objectives, and the fractal geometry theory has been proven to be powerful for the flow analysis in these media.

The tortuosity of pores is connected with the fractal properties of interstitial structure and it may be defined by a tortuosity factor being the ratio of the actual capillary tube length L_T to the length (thickness) of the interstitium L_0. In what follows we will limit the considerations to the interstitium being a matrix of capillary tubes.

The fractal scaling law for the tortuous capillary is as follows [25]

$$L_T = \frac{L_0^T}{(2r_c)^{T-1}} \tag{3.2}$$

where T is the fractal tortuosity factor the same as the classical tortousity factor given by Eq.(2.1).

Taking into account the above formula we may write for the pressure gradient [16, 17]

$$\frac{dp}{dy_T} = \frac{(2r_c)^{T-1}}{TL_0^{T-1}} \frac{dp}{dy}. \tag{3.3}$$

The cumulative size distribution of pores in the porous interstitium also follows the fractal scaling law (3.2) and it is given as [26-28]

$$N = \left(\frac{r_{c\,max}}{r_c}\right)^F \tag{3.4}$$

where $r_{c\,max}$ is the maximum pore (capillary) radius and F is fractal dimension for pores the same as in Eq.(3.1). Equation (3.4) leads to

$$dN = -\frac{F(r_{c\,max})^F}{r_c^{F+1}} dr_c ; \tag{3.5}$$

it follows from this expression that the number of pores decreases with the increase of pore sizes.

The area A^f of the porous interstitial matrix is now equal to

$$A^f = \frac{A_p}{\phi_p} = -\frac{1}{\phi_p} \int\limits_{r_{c\min}}^{r_{c\max}} \pi r_c^2 \, dN = \frac{F\pi r_{c\max}^2 \left(1 - \phi_p\right)}{(2 - F)\phi_p}$$ (3.6)

where A_p is the total pore area,

$$\phi_p = \phi_r^{2-F}$$ (3.7)

is now the fractal porosity [27] and

$$\phi_r = \frac{r_{c\min}}{r_{c\max}}, \qquad r_{c\min} \ll r_{c\max}.$$ (3.8)

In general, $r_{c\min}/r_{c\max} < 10^{-2}$ in fractal porous media [27, 28].

3.1. Fractal model of a Newtonian fluid flow through a porous interstitial matrix

The flow rate q through a single capillary tube of variable cross-section for a Newtonian fluid is given as follows (see also Eq.(2.4))

$$q(r_c) = \pi r_c^2 \, \upsilon_N\big|_{\phi_p = T = 1} = \frac{\pi r_c^4 \psi_N}{8\mu}\left(-\frac{dp}{dy_T}\right);$$ (3.9)

here the fractal tortuosity of a capillary tube was taken into account.

The total flow rate Q_N^f over matrix cross section can be obtained integrating Eq.(3.9) over the entire interval of pore sizes

$$Q_N^f = -\int\limits_{r_{c\min}}^{r_{c\max}} q(r_c)\, dN ;$$ (3.10)

taking into account Eqs (3.3), (3.5) and (3.8) we will obtain

$$Q_N^f = \frac{\pi \psi_N F r_{c\max}^{3+T}\left(1 - \phi_r^{3+T-F}\right)}{2^{4-T}\mu h^{T-1}T(3+T-F)}\left(-\frac{dp}{dy}\right)$$ (3.11)

here $L_0 = h$ is the thickness of the interstitial matrix (see Fig.3).
Note that the following inequalities hold for the epidermis as the porous matrix

$$1 < T < 2, \quad 0 < F < 2,$$

then the exponent $3 + T - F \geq 2$. In general, $\phi_r \approx 10^{-2}$, then $\phi_r^{3+T-F} << 1$. Hence Eq.(3.11) can be reduced to

$$Q_N^f = \frac{\pi \psi_N F r_{c\max}^{3+T}}{2^{4-T} \mu h^{T-1} T (3+T-F)} \left(-\frac{dp}{dy} \right).$$ (3.12a)

Dividing Eq.(3.12) by Eq.(3.6) gives the average velocity for the flow of a Newtonian fluid through the porous matrix

$$\upsilon_N^f = \frac{r_{c\max}^{1+T} (2-F) \phi_p \psi_N}{2^{4-T} \mu h^{T-1} T (3+T-F)(1-\phi_p)} \left(-\frac{dp}{dy} \right).$$ (3.13a)

It is easy to see that the fractal flow velocity of a Newtonian fluid through the porous interstitial matrix is more complicated than Eq.(2.1) describing the classical case of this flow. Equation (3.13a) is related not only to the characteristic parameter of the fluid such as viscosity μ but also to the structural parameters of the matrix such as: $h, r_{c\max}, \phi_p, T$ and F.

Note that Eqs (3.12a) and (3.13a) may also be written in the following forms

$$Q_N^f = Q_n \left(-\frac{dp}{dy} \right),$$ (3.12b)

and

$$\upsilon_N^f = \frac{Q_n}{A^f} \left(-\frac{dp}{dy} \right)$$ (3.13b)

where

$$Q_n = \frac{\pi \psi_N F r_{c\max}^{3+T}}{2^{4-T} \mu h^{T-1} T (3+T-F)}.$$

     To find the total amount of the interstitial fluid transported through the porous interstitial matrix evoked by the local thrust Δp provoked on the mucosa Eq.(2.5) can also be used.

3.2. Fractal model of the flow of a generalized Shulman viscoplastic fluid through a porous interstitial matrix

     Let us consider at first the flow of a generalized Shulman fluid with a large core through a porous interstitial matrix. The asymptotic flow rate q through a single tortuous capillary of variable cross-section is as follows

$$q(r_c) = \Upsilon^{\frac{m+3n}{n}} \frac{(-1)^{m+1}}{3 C_{m+3n}^m} \frac{\pi r_c^{\frac{m+3n}{n}} \psi_{Sh}}{2^{\frac{m}{n}} \mu} \left(-\frac{dp}{dy_T} \right)^{\frac{m}{n}}.$$ (3.14)

Introducing relationships (2.10)₁ and (3.3) into the above equation and integrating the result over a matrix cross-section we will obtain the total flow rate

$$Q_{Sh}^{f} = Q_{Lc}\left(-\frac{dp}{dy}\right)^{\frac{m}{n}} \tag{3.15}$$

Here all small quantities were neglected. Dividing Eq.(3.15) by Eq.(3.6) gives the asymptotic average fractal velocity for the flow of a Shulman fluid with a large core through a porous interstitial matrix

$$\upsilon_{Sh}^{f} = \frac{Q_{Lc}}{A^{f}}\left(-\frac{dp}{dy}\right)^{\frac{m}{n}}. \tag{3.16}$$

Expression for Q_{Lc} is presented in the Appendix. Both these formulae are important for m being an odd number.

Let us now consider the flow of a Shulman fluid with a small core through a porous matrix. The asymptotic flow rate q through a single tortuous capillary of variable cross-section is given as follows

$$q(r_{c}) = \left[1 - \frac{m(m+3n)}{m+3n-1}\Upsilon^{\frac{1}{n}}\right]\frac{\pi\psi_{Sh}nr_{c}^{\frac{m+3n}{n}}}{2^{\frac{m}{n}}(m+3n)\mu}\left(-\frac{dp}{dy_{T}}\right)^{\frac{m}{n}}. \tag{3.17}$$

Dealing here similarly as in the previous case we will obtain the total flow rate

$$Q_{Sh}^{f} = Q_{Sc}\left(-\frac{dp}{dy}\right)^{\frac{m}{n}}. \tag{3.18}$$

Here all small quantities were neglected. Dividing this equation by expression (3.6) gives the fractal average velocity for the Shulman fluid flow with small core through the porous matrix

$$\upsilon_{Sh}^{f} = \frac{Q_{Sc}}{A^{f}}\left(-\frac{dp}{dy}\right)^{\frac{m}{n}}. \tag{3.19}$$

Expression for Q_{Sc} is also presented in the Appendix.

These formulae are also important for all fluids derived from the Shulman fluid. Note that for the Bingham fluid we have $r_{0} \neq 0 \left(\Upsilon = \Upsilon_{min} \neq 0\right)$ and $m=n=1$; the formulae for the rate flow and the velocity will be, respectively

$$Q_{B}^{f} = Q_{BL}\left(-\frac{dp}{dy}\right), \tag{3.20}$$

$$\upsilon_{B}^{f} = \frac{Q_{BL}}{A^{f}}\left(-\frac{dp}{dy}\right), \tag{3.21}$$

for the flow with a large core and

$$Q_B^f = Q_{BS}\left(-\frac{dp}{dy}\right),$$ (3.22)

$$\upsilon_B^f = \frac{Q_{BS}}{A^f}\left(-\frac{dp}{dy}\right),$$ (3.23)

for the flow with a small core.

Flows of the power-law (Ostwald-de Waele) fluid are characterized by the following material parameters: $r_0 = 0\ (\Upsilon = \Upsilon_{\min} = 0)$ and $n=1$; taking into account formulae (3.18) and (3.19) we can write

$$Q_{0-w}^f = Q_{0-w}\left(-\frac{dp}{dy}\right)^m,$$ (3.24)

$$\upsilon_{0-w}^f = \frac{Q_{o-w}}{A^f}\left(-\frac{dp}{dy}\right)^m.$$ (3.25)

Expressions for Q_{BL}, Q_{BS} and Q_{0-w} are given in the Appendix. Note that the last formulae for $m=1$ represent the Newtonian fluid flow and they become the same as formulae (3.12) and (3.13)

3.3. Fractal models for pseudoplastic fluids

Let us consider at first the flow of the DeHaven fluid.
The flow rate q through a simple tortuous capillary of variable cross-section for a DeHaven fluid is as follows

$$q(r_c) = \frac{\pi r_c^4 \psi_N}{8\mu}\left(-\frac{dp}{dy_T}\right) + \frac{\pi k_i r_c^{n_i+4}\psi_a}{2^{n_i+1}\mu(n_i+4)}\left(-\frac{dp}{dy_T}\right)^{n_i+1}.$$ (3.26)

Introducing this equation into Eq.(3.10), after integration and taking into account Eqs (3.3), (3.5), (3.8), and neglecting the terms of small values, as a result we will obtain the following formula

$$Q_{DH}^f = Q_N^f + Q_A\left(-\frac{dp}{dy}\right)^{n_i+1}.$$ (3.27)

Dividing Eq.(3.27) by Eq.(3.6) gives the average velocity for the flow of the DeHaven fluid through the porous interstitial matrix

$$\upsilon_{DH}^f = \upsilon_N^f + \frac{Q_A}{A^f}\left(-\frac{dp}{dy}\right)^{n_i+1}$$ (3.28)

where Q_N^f and υ_N^f are given by Eqs (3.12) and (3.13), respectively.

It is easy to see that the fractal velocity of the DeHaven fluid through the porous matrix is related not only to the structural parameters of the matrix such as: $h, r_{c\max}, \phi_p, T$ and F and the pressure gradient but also to the characteristic parameters of the fluid: μ, k_i, n_i.

The flow rate q through a single tortuous capillary of variable cross-section for a Sisko fluid is given by the following formula

$$q\left(r_c\right) = \frac{\pi r_c^4 \psi_N}{8\mu}\left(-\frac{dp}{dy_T}\right) - \frac{\pi \mu_i r_c^{n_i+4}\psi_S}{2^{n_i+1}\left(n_i+4\right)\mu^{n_i+2}}\left(-\frac{dp}{dy_T}\right)^{n_i+1}. \tag{3.29}$$

Because Eqs (3.26) and (3.29) are similar we can also deal similarly with calculations. As a result we have

$$Q_S^f = Q_N^f - Q_S\left(-\frac{dp}{dy}\right)^{n_i+1}, \tag{3.30}$$

$$\upsilon_S^f = \upsilon_N^f - \frac{Q_S}{A_f}\left(-\frac{dp}{dy}\right)^{n_i+1}. \tag{3.31}$$

Expressions for Q_A and Q_S are given in the Appendix.

It can be see that in the case of this fluid the velocity depends not only on the structural parameters but on the characteristic parameters of the fluid which are now: μ, μ_i, n_i.

3.4. Fractal models for polar fluids

The asymptotic flow rate of a micropolar fluid through a fractal tortuous capillary tube is given as follows (see Eq.(2.21))

$$q\left(r_c\right) = \frac{\pi r_c^4 \psi_N}{8\mu}\left(\frac{\mu}{\mu+k}\right)\left(-\frac{dp}{dy_T}\right); \tag{3.32}$$

therefore the total flow rate Q_m^f over a matrix cross section will be (see Section (3.1))

$$Q_m^f = \frac{\pi \psi_N F r_{c\max}^{3+T}}{2^{4-T}\mu h^{T-1}T\left(3+T-F\right)}\left(\frac{\mu}{\mu+k}\right)\left(-\frac{dp}{dy}\right) \tag{3.33a}$$

whereas the average flow velocity

$$\upsilon_m^f = \frac{r_{c\max}^{1+T}\left(2-F\right)\psi_N \phi_p}{2^{4-T}\mu h_e^{T-1}T\left(3+T-F\right)\left(1-\phi_p\right)}\left(\frac{\mu}{\mu+k}\right)\left(-\frac{dp}{dy}\right). \tag{3.34a}$$

Note that the last equations may be written in the form

$$Q_m^f = Q_n\left(\frac{\mu}{\mu+k}\right)\left(-\frac{dp}{dy}\right), \tag{3.33b}$$

$$\upsilon_m^f = \frac{Q_n}{A^f}\left(\frac{\mu}{\mu+k}\right)\left(-\frac{dp}{dy}\right). \tag{3.34b}$$

Let us consider now the fractal velocity model for the flow of a couple-stress fluid. The asymptotic flow rate of this fluid through a fractal tortuous capillary tube is as follows (see Eq.(2.23))

$$q(r_c) = \frac{\pi r_c^4 \psi_N}{8\mu}\left[1 - \frac{4l^2}{r_c^2}\left(1 - \frac{\eta'}{\eta}\right)\right]\left(-\frac{dp}{dy_T}\right). \tag{3.35}$$

Applying the same procedure as in Section 3.1. we will obtain [16]

$$Q_{CS}^f = Q_N^f - \frac{\pi l^2 F r_{c\max}^{1+T}}{2^{2-T}\mu h^{T-1}T(1+T-F)}\left(1 - \frac{\eta'}{\eta}\right)\left(-\frac{dp}{dy}\right), \tag{3.36a}$$

whereas the average flow velocity is given by the formula

$$\upsilon_{CS}^f = \upsilon_N^f - \frac{l^2 r_{c\max}^{T-1}(2-F)\phi_p}{2^{2-T}\mu h^{T-1}T(1+T-F)(1-\phi_p)}\left(1 - \frac{\eta'}{\eta}\right)\left(-\frac{dp}{dy}\right); \tag{3.37a}$$

note that the last two formulae are only important for $1+T-F \geq 1$ (the case of $1+T-F=0$ is excluded). Writing the last equations in an abbreviated form we have

$$Q_{CS}^f = Q_N^f - Q_{C-S}\left(-\frac{dp}{dy}\right), \tag{3.36b}$$

and

$$\upsilon_S^f = \upsilon_N^f - \frac{Q_{CS}}{A^f}\left(-\frac{dp}{dy}\right) \tag{3.37b}$$

here

$$Q_{C-S} = \frac{\pi l^2 F r_{c\max}^{1+T}}{2^{2-T}\mu h^{T-1}T(1+T-F)}.$$

4. Classical and fractal permeability of the interstitium

For a sufficiently small porous region, such as interstitial areas being undergo of a mucosa subjected to thrust pressure, the fluid flow is described by the Darcy law, which - for a Newtonian fluid has the form [16]

$$\upsilon^i = \frac{\Phi_N^i}{\mu}\left(-\frac{dp}{dy}\right) \tag{4.1}$$

where the index i corresponds to

$$i \sim \begin{cases} c - \text{for classical flow,} \\ f - \text{for fractal flow;} \end{cases}$$

Φ_N^i is the coefficient of permeability.

Comparing this formula with Eqs (2.4) and (3.13) we find that:

-   for a classical Newtonian flow there is

$$\Phi_N^C = \frac{r_c^2 \varphi_p \psi_N}{8T} \tag{4.2}$$

-   whereas for a fractal Newtonian flow we have

$$\Phi_N^f = \frac{r_{c\max}^{1+T}(2-F)\phi_p \psi_N}{2^{4-T} h^{T-1} T(3+T-F)(1-\phi_p)} = \frac{\mu Q_n}{A^f}; \tag{4.3}$$

in the case of a straight capillary the tortuosity factor is equal to $T = 1$ and

$$\Phi_N^f = \frac{r_{c\max}^2 (2-F)\phi_p \psi_N}{8(4-F)(1-\phi_p)}. \tag{4.4}$$

It is easy to see that for a tortuous capillary system the fractal permeability of the interstitium depends on its thickness h and its fractal porosity ϕ_p, whereas for a straight capillary system this permeability only depends on its fractal porosity.

Note that the three - dimensional form given below is a more general form of the Darcy law

$$\mathbf{v}^i = \frac{\Phi_N^i}{\mu}(-\text{grad} p) \tag{4.5}$$

where: $\mathbf{v}^i$ is the velocity vector for classical flow $\left(\mathbf{v}^c\right)$ or for fractal flow $\left(\mathbf{v}^f\right)$.

For viscoplastic fluids described by a Shulman model the generalised form of the Darcy law is given as follows [17, 29]

$$\mathbf{v}^i = \frac{\Phi_{Sh}^i}{\mu}(-\text{grad} p)^{\frac{m}{n}} \tag{4.6}$$

where: Φ_{Sh}^i is the interstitial permeability for the Shulman fluid.

For a one-dimensional flow there is

$$\upsilon^i = \frac{\Phi_{Sh}^i}{\mu}\left(-\frac{dp}{dy}\right)^{\frac{m}{n}}. \tag{4.7}$$

For pseudoplastic fluids the generalisation of the Darcy law has the following forms [17]:

-   for the DeHaven fluid

$$\mathbf{v}^i_{DH} = \frac{\Phi^i_N}{\mu}\left(-\mathrm{grad}p\right) + \frac{\Phi^i_{DH}}{\mu}\left(-\mathrm{grad}p\right)^{n_i+1} \ , \tag{4.8}$$

in a one-dimensional flow there is

$$\upsilon^i_{DH} = \frac{\Phi^i_N}{\mu}\left(-\frac{dp}{dy}\right) + \frac{\Phi^i_{DH}}{\mu}\left(-\frac{dp}{dy}\right)^{n_i+1} \tag{4.9}$$

- for the Sisko fluid

$$\mathbf{v}^i_S = \frac{\Phi^i_N}{\mu}\left(-\mathrm{grad}p\right) - \frac{\Phi^i_S}{\mu}\left(-\mathrm{grad}p\right)^{n_i+1} \tag{4.10}$$

and in a one-dimensional flow

$$\upsilon^i_S = \frac{\Phi^i_N}{\mu}\left(-\frac{dp}{dy}\right) - \frac{\Phi^i_S}{\mu}\left(-\frac{dp}{dy}\right)^{n_i+1} . \tag{4.11}$$

For polar fluids the generalization of the Darcy law is as follows:
- for the micropolar fluid

$$\mathbf{v}^i_m = \frac{\Phi^i_N}{\mu}\left(\frac{\mu}{\mu+k}\right)\left(-\mathrm{grad}p\right) \tag{4.12}$$

whereas in a one-dimensional form

$$\upsilon^i_m = \frac{\Phi^i_N}{\mu}\left(\frac{\mu}{\mu+k}\right)\left(-\frac{dp}{dy}\right), \tag{4.13}$$

- for the couple-stress fluid

$$\mathbf{v}^i_{C-S} = \frac{\Phi^i_N - \Phi^i_{C-S}}{\mu}\left(-\mathrm{grad}p\right) \tag{4.14}$$

while in a one-dimension case

$$\upsilon^i_{C-S} = \frac{\Phi^i_N - \Phi^i_{C-S}}{\mu}\left(-\frac{dp}{dy}\right). \tag{4.15}$$

The coefficients Φ^i for all fluids under consideration are presented in Tab.2.

Table 2. Coefficients of permeability for considered fluids.

Model of fluid	Coefficient of permeability	
	Classical flow	Fractal flow
Newton	$$\Phi_N^C = \frac{r_c^2 \varphi_p \psi_N}{8T}$$	$$\Phi_C^f = \frac{\mu Q_n}{A^f}$$
Shulman	$$\Phi_{Sh}^C = T_{(n)}^{(m)} \frac{r_c^{\frac{m+3}{n}} \varphi_p \psi_{Sh}}{(2T)^{\frac{m}{n}}}$$	$$\Phi_{LC}^f = \frac{\mu Q_{Lc}}{A^f} \text{ for large core}$$ $$\Phi_{SC}^f = \frac{\mu Q_{Sc}}{A^f} \text{ for small core}$$
DeHaven	$$\Phi_{DH}^C = \frac{k_i r_c^{n_i+2} \varphi_p \psi_N \psi_A}{(2T)^{n_i+1}(n_i+4)}$$	$$\Phi_{DH}^f = \frac{\mu Q_A}{A^f}$$
Sisco	$$\Phi_S^C = \frac{\mu_i r_c^{n_i+2} \varphi_p \psi_N \psi_S}{(2T\mu)^{n_i+1}(n_i+4)}$$	$$\Phi_S^f = \frac{\mu Q_S}{A^f}$$
Couple-stress	$$\Phi_{CS}^C = \frac{l^2 \varphi_p \psi_N}{2T}$$	$$\Phi_{CS}^f = \frac{\mu Q_{C-S}}{A^f}$$

Conclusions

In this paper we have focused on an analytical description of mass transport through interstitial structures also called interstitium. Interstitium was modelled as a porous layer being a sponge porous matrix (SPM) in which the pores form tortuous capillaries of variable cross-sections.

Introducing a notion of the hydraulic radius

$$R_h = \frac{2A}{P}$$

where A is the non-circular capillary area, P is the capillary perimeter wetted by a flowing fluid, one may pass from the sponge capillary to the capillary tube of radius equal to $R_h = r_c$.

The interstitial space is filled out by thick collagen bundles which form complex lattices represented by network of capillaries. This structure creates the formation of a fractal system passing through the whole thickness of the interstitium.

The flow in this structure was analysed twofold: first, as classical flow, and next as fractal flow. Using the formulae for classical flow we present the new formulae for fractal flow. An input of hindrance factors allow us, in a simple procedure, to take into account the variability of the cross-sections of the capillaries or lymphangioles passing through the interstitium.

To make it possible to consider mass transport through the interstitial structure of the IFs in different consistence we presented the flow formulae for various models of fluids, such as: Newtonian, generalized second grade of the Shulman type, pseudoplastics and polar fluids.

Based on the theory of fractal geometry, the fractal expressions for the flow rate, flow velocity and fractal permeability for different fluids were presented. The proposed fractal models are expressed as functions of fluid characteristic parameters, structural parameters of the porous matrix and pressure gradient. The obtained results have a clear physical meaning and relate the properties of the fluids under consideration to the structural parameters of the porous matrix such as the interstitium.

It seems that the proposed improvements of the flow analysis in a porous bio-matrix broadens the general knowledge on the bio-flow and also allows further practical applications, e.g. an analysis of the flow through the cartilage of biobearings.

Appendix

Taking into account the considerations of Section 2.2 we will present the following auxiliary formulae.

Table A.1. Models of viscoplastic fluids.

Model of fluid	Form	Remarks
Shulman	$\tau = \left[\tau_0^{1/n} + \left(\mu\dot{\gamma} \right)^{1/m} \right]^n$	for *m=n*, Casson model
Casson	$\tau = \left[\tau_0^{1/n} + \left(\mu\dot{\gamma} \right)^{1/n} \right]^n$	for *n=2*, simple model of Casson
Vočadlo	$\tau = \left[\tau_0^{1/n} + \mu\dot{\gamma} \right]^n$	it is sometimes called Robertson-Stiff model
Herschel-Bulkley	$\tau = \tau_0 + \left(\mu\dot{\gamma} \right)^{1/m}$	for *m=1*, Bingham model
Bingham	$\tau = \tau_0 + \mu\dot{\gamma}$	

Here τ is the shear stress, τ_0 is the yield shear stress, $\dot{\gamma}$ is the shear strain rate, μ is the plastic viscosity (consistency factor).

To find three-dimensional forms of the stress tensor $\boldsymbol{T}$, corresponding to the above given one-dimensional forms of τ, we may use the following formulae [16]

if $\qquad \tau = f\left(\dot{\gamma}\right)\dot{\gamma}, \qquad$ then $\qquad \boldsymbol{T} = -p\boldsymbol{I} + \boldsymbol{\Lambda}$

where $\qquad \boldsymbol{\Lambda} = f\left(A\right)\boldsymbol{A_1}, \qquad\qquad A = \left[\frac{1}{2}\mathrm{tr}\left(\boldsymbol{\Lambda_1^2}\right) \right]^{1/2}.$

The equations of motion of generalized second grade fluids are as follows

$$\mathrm{div}\,\mathbf{v} = 0,$$

$$\rho\frac{d\mathbf{v}}{dt} = \rho\boldsymbol{f} + \mathrm{div}\,\boldsymbol{T}$$

where $\boldsymbol{T}$ depends now on a model of the fluid. Let us assume here two models proposed by Walicki and Walicka in 1998, based on the Shulman model of plastic viscosity. Thus, we have two constitutive equations:

- for model I

$$\boldsymbol{T} = -p\boldsymbol{I} + M\boldsymbol{A_1} + \alpha_1\boldsymbol{A_1^2} + \beta_1\boldsymbol{A_2},$$

- for model II

$$\boldsymbol{T} = -p\boldsymbol{I} + M\left(\boldsymbol{A_1} + \alpha_2\boldsymbol{A_1^2} + \beta_2\boldsymbol{A_2} \right),$$

where

$$M = \left[\tau_0^{\frac{1}{n}} + \left(\mu A\right)^{\frac{1}{m}} \right]^n A^{-1}, \qquad A = \left[\frac{1}{2}\mathrm{tr}\left(\boldsymbol{A_1^2}\right) \right]^{1/2},$$

here $\boldsymbol{A_1}$ and $\boldsymbol{A_2}$ are the first two Rivlin-Ericksen kinematic tensors defined by

$$A_1 = 2D = \left(\nabla \mathbf{v} + \nabla \mathbf{v}^T \right), \qquad A_2 = \dot{A}_1 + A_1 \nabla \mathbf{v} + \nabla \mathbf{v}^T A_1$$

and $\alpha_i, \beta_i \ (i = 1, 2)$ are material constants.

Now, if we define a modified pressure p through

$$p = p_{Sh} - \left(\alpha_i + 2\beta_i \right) M^{j-1} \left(\frac{d\upsilon}{dr} \right)^2$$

where $j=1$ for model I, $j=2$ for model II, we will obtain Eq.(2.8) for the average velocity flow through capillary tube. For $\alpha_i = \beta_i = 0 \ (p = p_{Sh})$ we have the flow of the Shulman fluid and Eq.(2.8) is correct. Now, we present two auxiliary tables for Section 2.3.

Table A.2. Models of fluids similar to the DeHaven fluid model.

Author(s)	Original model	Model taken into account	κ_i	Comments
$n_i = n$				"$n+1$" power models
DeHaven	$\mu_0 \dot{\gamma} = \tau \left(1 + \kappa |\tau|^n \right)$	$-$	κ	
Meter	$\tau = \left[\mu_\infty + \dfrac{\mu_0 - \mu_\infty}{1 + (\kappa\tau)^n} \right] \dot{\gamma}$	$\mu_0 \dot{\gamma} = \tau \left(1 + \dfrac{\mu\kappa^n}{\mu_0} \tau^n \right)$	$\dfrac{\mu\kappa^n}{\mu_0}$	$\mu = \mu_0 - \mu_\infty$
$n_i = n - 1$				"n" power model
Ellis	$\tau = \dfrac{\mu_0 \dot{\gamma}}{1 + \kappa |\tau|^{n-1}}$	$\mu_0 \dot{\gamma} = \tau \left(1 + \kappa |\tau|^{n-1} \right)$	κ	
$n_i = 2$				"Cubic" models
Rotem-Shinnar	$\tau = \dfrac{\mu_0 \dot{\gamma}}{1 + \sum\limits_i^n \kappa_i \tau^{2i}}$	$\mu_0 \dot{\gamma} = \tau \left(1 + \kappa\tau^2 \right)$	κ	The model has a practical meaning for $i = 1$
Ree-Eyring	$\tau = \mu_0 \dot{\gamma} \left[\dfrac{\sinh(\kappa\tau)}{(\kappa\tau)} \right]^{-1}$	$\mu_0 \dot{\gamma} = \tau \left(1 + \dfrac{\kappa^2}{6} \tau^2 \right),$	$\dfrac{\kappa^2}{6}$	
Rabinowitsch	$\tau = \dfrac{\mu_0 \dot{\gamma}}{1 + \kappa\tau^2}$	$\mu_0 \dot{\gamma} = \tau \left(1 + \kappa\tau^2 \right)$	κ	
Reiner-Philippoff	$\tau = \left[\mu_\infty + \dfrac{\mu_0 - \mu_\infty}{1 + (\kappa\tau)^2} \right] \dot{\gamma}$	$\mu_0 \dot{\gamma} = \tau \left(1 + \dfrac{\mu\kappa^2}{\mu_0} \tau^2 \right)$	$\dfrac{\mu\kappa^2}{\mu_0}$	$\mu = \mu_0 - \mu_\infty$
$n_i = 1$				"Quadratic" models
Peek-McLean	$\tau = \left[\mu_\infty + \dfrac{\mu_0 - \mu_\infty}{1 + (\kappa\tau)} \right] \dot{\gamma}$	$\mu_0 \dot{\gamma} = \tau \left(1 + \dfrac{\mu\kappa}{\mu_0} \tau \right)$	$\dfrac{\mu\kappa}{\mu_0}$	$\mu = \mu_0 - \mu_\infty$
Seely	$\tau = \left[\mu_\infty + \dfrac{\mu_0 - \mu_\infty}{e^{(\kappa\tau)}} \right] \dot{\gamma}$	$\mu_0 \dot{\gamma} = \tau \left(1 - \dfrac{\mu\kappa}{\mu_0} \tau \right)$	$-\dfrac{\mu\kappa}{\mu_0}$	$\mu = \mu_0 - \mu_\infty$

Table.1.3. Model of fluids similar to the Sisko fluid model.

Author(s)	Model	Reduced model	μ_i	Comments
$n_i = n$				"n+1" power models
Sisko	$\tau = \left[\mu_0 + \mu \lvert \dot{\gamma} \rvert^n \right] \dot{\gamma}$	–	μ	
Carreau-Yasuda	$\tau = \left\{ \mu_\infty + \dfrac{\mu_0 - \mu_\infty}{\left[1 + (\kappa\dot{\gamma})^n \right]^{\frac{\alpha}{n}}} \right\} \dot{\gamma}$	$\tau \approx \left[\mu_0 - \dfrac{\alpha\mu}{n}(\kappa\dot{\gamma})^n \right]\dot{\gamma}$; $\mu = \mu_0 - \mu_\infty$	$-\dfrac{\alpha\mu\kappa^n}{n}$	Cross model for $\alpha = n$ Williamson-Moore model for $\alpha = n = 1$
Elsharkawy-Hamrock	$\tau = \dfrac{\mu_0 \dot{\gamma}}{\left[1 + (\kappa\dot{\gamma})^n \right]^{\frac{1}{n}}}$	$\tau \approx \left[\mu_0 - \dfrac{\mu_0}{n}(\kappa\dot{\gamma})^n \right]\dot{\gamma}$	$-\dfrac{\mu_0\kappa^n}{n}$	
$n_i = 2$				"Cubic" models
Prandtl	$\tau = \mu_0 \dfrac{\arcsin(\kappa\dot{\gamma})}{(\kappa\dot{\gamma})} \dot{\gamma}$	$\tau \approx \left[\mu_0 + \dfrac{\mu_0}{6}(\kappa\dot{\gamma})^2 \right]\dot{\gamma}$	$\dfrac{\mu_0\kappa^2}{6}$	
Eyring-Sutterby	$\tau = \mu_0 \left[\dfrac{\operatorname{arsinh}(\kappa\dot{\gamma})}{\kappa\dot{\gamma}} \right]^n \dot{\gamma}$	$\tau \approx \left[\mu_0 - \dfrac{n\mu_0}{6}(\kappa\dot{\gamma})^2 \right]\dot{\gamma}$	$-\dfrac{n\mu_0\kappa^2}{6}$	Prandtl-Eyring model for $n = 1$
Sutterby	$\tau = \left\{ \mu_\infty + (\mu_0 - \mu_\infty) \times \right.$ $\left. \left[\dfrac{\operatorname{arsinh}(\kappa\dot{\gamma})}{\kappa\dot{\gamma}} \right]^n \right\} \dot{\gamma}$	$\tau \approx \left[\mu_0 + \dfrac{n\mu}{6}(\kappa\dot{\gamma})^2 \right]\dot{\gamma}$; $\mu = \mu_0 - \mu_\infty$	$-\dfrac{n\mu\kappa^2}{6}$	Powell-Eyring model for $n = 1$
Gecim-Winer	$\tau = \mu_0 \left[\dfrac{\tanh(\kappa\dot{\gamma})}{(\kappa\dot{\gamma})} \right] \dot{\gamma}$	$\tau \approx \left[\mu_0 - \dfrac{\mu_0}{3}(\kappa\dot{\gamma})^2 \right]\dot{\gamma}$	$-\dfrac{\mu_0\kappa^2}{3}$	
$n_i = 1$				"Quadratic" models
Bair-Winer	$\tau = \mu_0 \left(\dfrac{1 - e^{-\kappa\dot{\gamma}}}{\kappa\dot{\gamma}} \right) \dot{\gamma}$	$\tau \approx \left[\mu_0 - \dfrac{\mu_0}{2}(\kappa\dot{\gamma}) \right]\dot{\gamma}$	$-\dfrac{\mu_0\kappa}{3}$	

Considering the flow of a micropolar fluid in a capillary tube (see Section 2.4) we have the following expression for the straight capillary [16]

$$\upsilon_m = \frac{r_c^2}{4(2\mu + k)}(1 - \beta m)\left(-\frac{dp}{dy} \right)$$

where

$$p_m = \frac{2\phi I_2(M)}{M\, I_1(M)}, \quad M = m r_c, \quad \phi = \frac{k}{\mu + k}, \quad m = \left(\frac{2\mu + k}{\mu + k} \cdot \frac{k}{\gamma} \right)^{1/2}$$

and γ is the spin viscosity coefficient, whereas $I_1(M), I_2(M)$ are the modified Bessel functions of the first and second order and the first kind, respectively.

This expression is correct for all values of M; for small values of M it will be

$$\upsilon_m = \frac{r_c^2}{8\mu}\left(\frac{\mu}{\mu+k}\right)\left(-\frac{dp}{dy}\right).$$

Considering the flow of a couple-stress fluid in a capillary tube (see Section 2.4) we have the following expression for the straight capillary [16]

$$\upsilon_{C-S} = \frac{r_c^2}{8\mu}\left(1-\beta_{CS}\right)\left(-\frac{dp}{dy}\right)$$

where

$$\beta_{CS} = -\frac{4(\eta-\eta')I_2(\psi)}{\psi\left[\eta\psi I_0(\psi)-(\eta+\eta')I_1(\psi)\right]} \approx -\frac{4(\eta-\eta')}{\eta\psi^2}, \qquad \psi = \frac{r_c}{l}.$$

Taking into account the considerations of Section 3.2 we will present in what follows all auxiliary formulae

$$Q_{Lc} = \frac{(-1)^{m+1}}{3C_{m+3n}^m} \frac{\psi_{Sh}Fr_{c\max}^{1+\frac{m}{n}T}\Upsilon_{\min}^{\frac{m+3n}{n}}}{2^{\frac{m}{n}(2-T)}\mu T^{\frac{m}{n}}h^{\frac{m}{n}(T-1)}\left[\frac{m}{n}(T-1)-F\right]}$$

where $\qquad \Upsilon_{\min} = \frac{r_0}{r_{c\max}},$

$$Q_{Sc} = \left[1 - \frac{m(m+3n)\left(3+\frac{m}{n}T-F\right)}{(m+3n-1)\left(3+\frac{mT-1}{n}-F\right)}\Upsilon_{\min}^{\frac{1}{n}}\right]\frac{\psi_{Sh}nFr_{c\max}^{3+\frac{m}{n}T}}{2^{\frac{m}{n}(2-T)}(m+3n)\mu T^{\frac{m}{n}}h^{\frac{m}{n}(T-1)}\left(3+\frac{m}{n}T-F\right)},$$

$$Q_{BL} = \frac{1}{3C_4^1}\frac{\pi\psi_B Fr_{c\max}^{3+T}\gamma_{\min}^4}{2^{2-T}\mu Th^{T-1}(T-1-F)},$$

$$Q_{BS} = \left[1 - \frac{4(3+T-F)}{3(2+T-F)}\gamma_{\min}\right]\frac{\pi\psi_B Fr_{c\max}^{3+T}}{2^{4-T}\mu Th^{T-1}(3+T-F)},$$

$$Q_{0-W} = \frac{\pi\psi_{0-W}Fr_{c\max}^{3+mT}}{2^{m(2-T)}(m+3)\mu T^m h^{m(T-1)}(3+T-F)}.$$

Taking into account the considerations of Section 3.3 we will present in what follows the auxiliary formulae

$$Q_A = \frac{\pi \psi_a k_i F r_{c\max}^{3+(n_i+1)T}}{2^{(n_i+1)(2-T)} \mu (n_i + 4) h^{(n_i+1)(T-1)} T^{n_i+1} \left[3 + (n_i + 1)T - F \right]},$$

$$Q_S = \frac{\pi \psi_S \mu_i F r_{c\max}^{3+(n_i+1)T}}{2^{(n_i+1)(2-T)} \mu^{n_i+2} (n_i + 4) h_e^{(n_i+1)(T-1)} T^{n_i+1} \left[3 + (n_i + 1)T - F \right]}.$$

Nomenclature

A	– area
A^f	– area of porous interstitial matrix
A_p	– fractal pore area
F	– fractal dimension of an object
h	– thickness
k	– vortex viscosity
k_i	– material coefficient for a DeHaven fluid
L_0	– nominal capillary length
L_T	– actual (tortuous) capillary length
m,n	– power exponents for Shulman fluids
N	– number of pores
n_i	– power exponents for pseudoplastic fluids
P	– wetted perimeter of a fissure
p	– pressure
Q	– total flow rate
q	– capillary flow rate
R_h	– hydraulic radius
r_c	– capillary radius
T	– fractal tortuosity factor
$T_{(n)}^{(m)}$	– polynomial function for a Shulman fluid
υ	– flow velocity
$\mathbf{v}$	– velocity vector
α_i, β_i	– material constants for Rivlin-Ericksen fluids
γ	– spin
$\dot{\gamma}$	– shear strain rate
η, η'	– additional couple-stress factors
μ	– shear or plastic viscosity
μ_i	– material coefficient for a Sisko fluid
τ	– shear stress
Φ^i	– coefficient of permeability
φ_p	– classical porosity
ϕ_p	– fractal porosity
ϕ_r	– radii ratio
ψ	– hindrance factor
Υ	– relative core flow radius

Abbreviations

CL	– collagen
CTCs	– circulating tumor cells
ECMs	– extracellular matrices
EL	– elastin
FN	– fibronectin
GAGs	– glycosaminoglycans
GPs	– glycoproteins
HA	– hyaluronate
IF	– interstitial fluid
IFP	– interstitial fluid pressure
ISMs	– interstitial matrices
ISs	– interstitial structures
LAs	– laminis
PCMs	– pericellular matrices
PGs	– proteoglicans

References

[1] Frantz C., Stewart K.M. and Weaver V.M. (2010): *The extracellular matrix at a glance.* – J. Cell. Sci., vol.123, pp.4195-4200.

[2] Clause K.C. and Barker T.H. (2013): *Extracellular matrix signaling in morphogenesis and repair.* – Cur. Opin. Biotechnol., vol.24, pp.830-833.

[3] Bonnas C., Chou J. and Werb Z. (2014): *Remodeling the extracellular matrix in development and disease.* – Nature Reviews. Molecular Cell Biology, vol.15, No.12, pp.786-801.

[4] Theocharis A.D., Skandalis S.S., Gialeli C. and Karamanos N.K. (2016): *Extracellular matrix structure.* – Adv. Drug Delivery Rev., vol.97, No.1, pp.4-27.

[5] Michel G., Tonon T., Scornet D., Cock J.M. and Kloareg B. (2010): *The cell wall polysacchariel metabolism of the brown alga ectocarpus siliculosus. Insights into the evolution of extracellular matrix polysaccharides in eukaryotes.* – New Phytologist, vol.188, No.1, pp.82-97.

[6] Benias P.C., D'Souza L.S., Papafragkakis H., Kim J., Harshan M., Theise N.D. and Carr-Locke D.L. (2016): *Needle-based confocal endomicroscopy for evaluation of malignant lymph nodes - a feasibility study.* – Endoscopy, vol.48, No.4, pp.923-928.

[7] Benias P.C., Wells R.G., Sackey-Aboagye B., Klavan H., Reidy J., Buonocore D., Miranda M., Kornacki S., Wayne M., Carr-Locke D.L. and Theise N.D. (2018): *Structure and distribution of an unrecognized interstitium in human tissues.* – Sci. Reports, 8:4947/Doi:10:1038/s41598-018-23062-6.

[8] Wiig H. and Swartz M.A. (2012): *Interstitial fluid and lymph formation and transport; physiological regulation and roles in inflamation and cancer.* – Phys. Rev., vol.92, No.3, pp.1005-1060.

[9] Eckhouse S.R. and Spinale F.G. (2012): *Changes in the myocardial interstitium and contribution to the progression of the heart failure.* – Heart Fail Clin., vol.8, No.1, pp.7-20.

[10] Loeser C.S., Robert M.E., Mennene A., Nathanson M.H. and Jarnidar P. (2011): *Confocal endermicroscopic examination of malignant biliary structures and histologic correlation with limphatics.* – J. Clin Gastroenterol , vol.45, pp.246-252.

[11] Berggreen E. and Wiig H. (2014): *Lymphatic function and responses in periodontal disease.* – Exp. Cell Res., vol.325, No.2, pp.130-137.

[12] Louvean A., Smirnov I., Keves T.J., Eccles J.D., Rouhani S.J., Peske J.D. Derecki N.C., Castle D., Mandell J.W., Lee K.S., Harris T.H. and Kipnis J. (2015): *Structural and functional features of central nervous system lymphatic vessels.* – Nature, vol.523, pp.337-341.

[13] Zeisberg M. and Kalluri R. (2015): *Physiology of the renal interstitium*. – Clin. J. Am. Soc. Nephrol., vol.10, No.10, pp.1831-1840.

[14] de Wit S., van Dalum G. and Terstappe L.W. (2014): *Detection of circulating tumor cells*. – Scientifica, Doi: 10.1155/2014/819362.

[15] Auang Q., Wang Y., Chen X., Wang Y.., Li Z., Du S., Wang L. and Chen S. (2018): *Nanotechnology - based strategies for early cancer diagnosis using circulation tumor cells as a liquid biopsy*. – Nanotheranostics, vol.2, No.1, pp.21-41.

[16] Walicka A. (2017): *Rheology of Fluids in Mechanical Engineering*. – Zielona Góra University Press.

[17] Walicka A. and Iwanowska-Chomiak B. (2018): *Fractal model of the transdermal drug delivery*. – Int. J. Appl. Mech. Eng., vol.23, No.4, pp.989-1004.

[18] Walicka A., Falicki J. and Iwanowska-Chomiak B. (2019): *Rheology of drugs for topical and transdermal delivery*. – Int. J. Appl. Mech. Eng., vol.24, No.1, pp.179-198.

[19] Walicka A. (2018a): *Simulation of the flow through porous layer composed of converging - diverging capillary fissures and tubes*. – Int. J. Appl. Mech. Eng., vol.23, No.1, pp.161-185.

[20] Walicka A. (2018b): *Flows of Newtonian and power-law fluids in symmetrically corrugated fissures and tubes*. – Int. J. Appl. Mech. Eng., vol.23, No.1, pp.187-215.

[21] Walicka A., Jurczak P. and Falicki J. (2018): *Flows of Sisko fluid through symmetrically curved capillary fissures and tubes*. – Machine Dynamics Research, vol.42, No.3, pp.27-54.

[22] Walicka A., Walicki E., Jurczak P. and Falicki J. (2018): *Effect of hindrance factors on a squeeze film of a porous bearing with a DeHaven fluid*. – Machine Dynamics Research, vol.42, No.1, pp.15-33.

[23] Mandelbrot B.B. (1967): *How long is the coast of Britain? Statistical self-similarity and fractional dimension*. – Science, vol.155, pp.636-638.

[24] Mandelbrot B.B. (1982): *The Fractal Geometry of Nature*. – New York: W.H. Freeman.

[25] Wheateraft S.W. and Tyler S.W. (1988): *An explanation of scale-dependent dispersivity in heterogeneous aquifers using concepts of fractal geometry*. – Water Resour. Res., vol.24, pp.566-578.

[26] Yu B.M. and Li J.H. (2001): *Some fractal characters of porous media*. – Fractals, vol.9, No.3, pp.365-372.

[27] Yu B.M. and Cheng P. (2002): *A fractal model for permeability of bi-dispersed porous media*. – Int. J. Heat Mass Transfer, vol.45, No.14, pp.2983-2993.

[28] Yu B.M. (2005): *Fractal character for tortuous stream tubes in porous media*. – Chin. Phys. Lett., vol.22, No.1, pp.158-160.

[29] Walicki E. (2005): *Rheodynamics of Slide Bearings Lubrication* (in Polish). – Zielona Góra: University Press.